Theoretical study of stereodynamics for the reaction $O(^3P) + D_2$ ($v = 0$, $j = 0$) $\rightarrow$ OD+D and isotope effect

Xu Zeng-Hui(许增慧) and Zong Fu-Jian(宗福建)†

School of Physics, Shandong University, Jinan 250100, *China*

(Received 17 October 2010; revised manuscript received 25 December 2010)

Quasi-classical trajectory (QCT) calculations have been performed to study the product polarization behaviours in the reaction $O(^3P) + D_2$ ($v = 0$, $j = 0$) $\rightarrow$ OD + D. By running trajectories on the $^3A'$ and $^3A''$ potential energy surfaces (PESs), vector correlations such as the distributions of the polarization-dependent differential cross sections (PDDCSs), the angular distributions of $P(\theta_r)$ and $P(\phi_r)$ are presented. Isotope effect is discussed in this work by a comprehensive comparison with the reaction $O(^3P) + H_2$ ($v = 0$, $j = 0$) $\rightarrow$ H + H. Common characteristics as well as differences are discussed in product alignment and orientation for the two reactions. The isotope mass effect differs on the two potential energy surfaces: the isotope mass effect has stronger influence on $P(\theta_r)$ and PDDCSs of the $^3A'$ PES while the opposite on $P(\phi_r)$ of the $^3A''$ potential energy surface.

Keywords: chemical stereodynamics, quasiclassical trajectory calculation, isotope effect, vector correlation

PACS: 31.15.xv, 34.20.–b, 82.20.Kh **DOI:** 10.1088/1674-1056/20/6/063104

1. Introduction

In recent years, chemical reaction dynamics has become an important field that attracts much more attention all over the world.[1−35] Due to its significant effects in atmosphere reaction, the reaction $O + H_2$ has extensively attracted much attention of many researchers.[1−26] Lots of studies have been reported about the reaction for its significance in chemistry. Consequently throughout the recent decades, advances about this reaction and its isotope variants $O + D_2$/DH/HD have been obtained by generations of researchers both theoretically and experimentally. In theoretical fields, quantum dynamical method and quasi-classical trajectory (QCT) method are the two methods that have been mainly applied to investigate the characteristics of the reaction $O + H_2$.[1−26]

From the theoretical side, considerable studies on this reaction have been done in past twenty years.[1−26] In 2004, Braunstein *et al.*[4] reported the results of time-dependent quantum mechanics (TDQM) and QCT studies of the excitation function for $O(^3P) + H_2$ ($v = 0$, 1, 2, 3, $j = 0$) from threshold to 30-kcal/mol collision energy using benchmark potential energy surfaces of Rogers's. They found that for H_2 ($v = 0$) there is excellent agreement between quantum and classical results. The TDQM results show that the reactive threshold drops from 10 kcal/mol ($v = 0$) to 6 kcal/mol ($v = 1$), 5 kcal/mol ($v = 2$) and 4 kcal/mol ($v = 3$) respectively, suggesting a much slower increase in rate constant with vibrational excitation above $v = 1$ than below. For H_2 ($v > 0$), the classical results are larger than the quantum results by a factor ~ 2 near the threshold, but the agreement monotonically improves until they are within ∼10% near 30-kcal/mol collision energy. They also computed QCT OH (v', j') state-resolved cross sections and angular distributions. The QCT state-resolved OH (v') cross sections peak at the same vibrational quantum number as the H_2 reagent. The OH rotational distributions are also quite hot and tend to cluster around high rotational quantum numbers. In 2006, Wang *et al.*[5] investigated the reaction $O\left(^3P\right) + H_2$ ($v = 0$, $j = 0$) with both QCT and accurate quantum dynamical methods on the potential energy surfaces (PESs) of BMS1 (Brandão–Mogo–Silva) and BMS2 which are extended from PESs of the lowest triplet electronic state of Rogers', in order to study the possible influence of the van der Waals forces on the reaction $O\left(^3P\right) + H_2$ ($v = 0$, $j = 0$). Their QCT calculations revealed that for collisions near the threshold, the reaction is sensitive to the van der Waals region while the quantum dynamic results clearly show that

†Corresponding author. E-mail: fjzong@sdu.edu.cn

© 2011 Chinese Physical Society and IOP Publishing Ltd

the reaction mainly occurs through tunneling.

However, many previous studies are limited to scalar properties. In order to obtain almost complete information about the dynamical characteristics of the reaction, vector properties should be considered as well. Vector properties, such as velocities and angular momentum, possess not only magnitudes that can be directly related to translational and rotational energies but also well-defined directions.[6] Recent years, some researchers commence to investigate not only scalar properties but also vector properties.[7−9,15,19−20,26] In 2009, Chen *et al.*[7] studied the reaction $\mathrm{O}\left(^1\mathrm{D}\right) + \mathrm{H_2}$ (v = 0, 1, 2, 3, j = 0) using QCT method on the DK (Dobbyn and Knowles) PES, they obtained vector correlation information which shows that the product alignment is sensitive to the reactant vibrational quantum number (v) at collision energy of 19 kcal/mol. Moreover, backward scattering becomes weaker and forward scattering acts conversely with increasing value of v. Liu *et al.*[8] carried out the dynamics calculations of the reactions $\mathrm{O}\left(^1\mathrm{D}\right) + \mathrm{H_2/D_2/HD}$ by QCT method with symplectic integration on the ground state $^1\mathrm{A}'$ PES given by Dobbyn and Knowles. Vector correlations were presented and their results showed that the intermediate geometrical structures and lifetimes of the reactive collisions play a vital role in these reactions. Hou *et al.*[9] also studied the stereodynamics of the reaction $\mathrm{O}\left(^1\mathrm{D}\right) + \mathrm{D_2}$ on $^1\mathrm{A}'$ and $^3\mathrm{A}''$ PESs given by Dobbyn and Knowles with QCT method, especially the vector correlations between products and reagents. More recently in 2010, Han *et al.*[10] investigated the reaction $\mathrm{H\,(D) + FO}$ (v = 0, j = 0) on a recent PES of $^3\mathrm{A}''$ electronic state given in Ref. [25], the vector properties such as the distributions of the polarization-dependent differential cross sections (PDDCSs), the angular distributions of $P(\theta_r)$ and $P(\phi_r)$ are also considered as significant aspects.

In our previous work,[26] we applied the QCT method to study the reaction $\mathrm{O}(^3\mathrm{P}) + \mathrm{H_2}$ (v = 0, j = 0) $\rightarrow$ OH + H on the $^3\mathrm{A}'$ and $^3\mathrm{A}''$ PESs described by Rogers *et al.*[18] In that work we compared the product polarizations for the two triplet states and on the new versions of the triplet PES of Rogers *et al.*[18] comprehensively and extensively. In order to study the isotope effect and the influence of different PESs to the product polarization, we extend our previous work to the reaction $\mathrm{O}(^3\mathrm{P}) + \mathrm{D_2}$ (v = 0, j = 0) $\rightarrow$ OD + D on the same PESs using the same method. Comparisons have been made between the two isotope variant reactions and the reasons leading to the distinction will also be inferred. Section 2 concisely introduces the theories and methods for chemical stereodynamics. Section 3 gives calculated results and discussion. Section 4 presents the conclusions.

2. Theories and methods

2.1. Product rotational polarization

Here we introduce the center-of-mass (CM) reference frame to describe the distributions of the vectors $\boldsymbol{k}$, $\boldsymbol{k}'$, and $\boldsymbol{j}'$. A series of PDDCSs can be used to describe the fully correlated angular distributions of $\boldsymbol{k}$, $\boldsymbol{k}'$, and $\boldsymbol{j}'$ in the CM frame. Figure 1 is the brief sketch map of the CM frame we use. The reagents initial relative velocity vector $\boldsymbol{k}$ is parallel to the z axis. The y axis is perpendicular to the x–z plane which contains the reagents initial and products final relative velocities vectors, $\boldsymbol{k}$ and $\boldsymbol{k}'$. Angle θ_t is the angle between $\boldsymbol{k}$ and $\boldsymbol{k}'$ (so-called scattering angle); ϕ_r and θ_r are the polar and azimuthal angles of the final rotational angular momentum $\boldsymbol{j}'$.

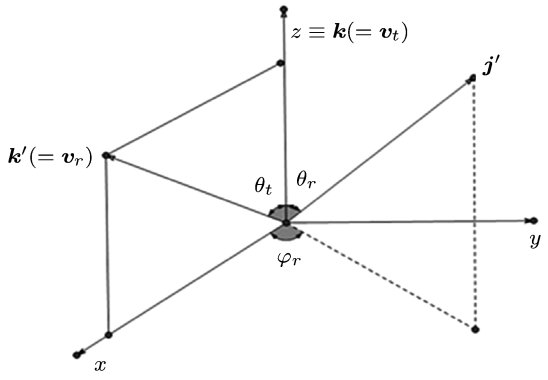


Fig. 1. The CM frame used to describe the stereodynamical behaviours of a chemical reaction.

The distribution function $P(\theta_r)$ describing $\boldsymbol{k}$–$\boldsymbol{j}'$ correlation can be expanded into a series of Legendre polynomials as[27−30]

$$P(\theta_r) = \frac{1}{2}\sum_k (2k+1) a_0^{(k)} P_k(\cos\theta_r), \tag{1}$$

$$\begin{aligned} a_0^{(k)} &= \int_0^{\pi} P(\theta_r) P_k(\cos\theta_r) \sin\theta_r \mathrm{d}\theta_r \\ &= \langle P_k(\cos\theta_r)\rangle. \end{aligned} \tag{2}$$

The coefficient $a_0^{(k)}$ is called polarization parameter. The acute bracket indicates an average to all the reactive trajectories. When $P(\theta_r)$ is expanded up to $k = 18$, it will show a good convergence.

The dihedral angle distribution function $P(\phi_r)$ describing $\boldsymbol{k}$–$\boldsymbol{k}$–$\boldsymbol{j}'$ correlation can be expanded into Fourier series as[27−30]

$$P(\phi_r) = \frac{1}{2\pi}\Bigg(1 + \sum_{n_{\rm evne}\geq 2} a_n \cos n\phi_r + \sum_{n_{\rm odd}\geq 1} b_n \sin n\phi_r\Bigg), \quad (3)$$

$$a_n = 2\langle \cos n\varphi_r\rangle, \quad b_n = 2\langle \sin n\varphi_r\rangle. \quad (4)$$

And $P(\varphi_r)$ shows an ideal convergence when it expands up to $n = 24$.

Generally, θ_r and ϕ_r are used to define the direction of $\boldsymbol{j}'$ and the distribution of product rotational momentum $P(\theta_r\phi_r)$ can be expanded as[27−30]

$$P(\theta_r, \phi_r) = \frac{1}{4\pi}\sum_{kq}[k]a_q^k C_{kq}(\theta_r, \phi_r)^* = \frac{1}{4\pi}\sum_k\sum_{q\geq 0}[a_{q\pm}^k \cos q\phi_r - a_{q\mp}^k \,{\rm i}\sin q\phi_r]C_{kq}(\theta_r, 0), \quad (5)$$

in which the parameter a_q^k can be obtained from the following equations

$$a_{q\pm}^k = 2\left\langle C_{k|q|}(\theta_r, 0)\cos q\phi_r\right\rangle, \quad k \text{ is even}, \quad (6)$$

$$a_{q\pm}^k = 2\,{\rm i}\left\langle C_{k|q|}(\theta_r, 0)\sin q\phi_r\right\rangle, \quad k \text{ is odd}. \quad (7)$$

In calculations $P(\theta_r\phi_r)$ has a good convergence when expanded up to $k = 7$.

The fully correlated angular distribution can be written as[27,29,30]

$$P(\omega_t, \omega_r) = \sum_{kq}\frac{[k]}{4\pi}\frac{1}{\sigma}\frac{{\rm d}\sigma_{kq}}{{\rm d}\omega_t}C_{kq}(\theta_r, \phi_r)^*, \quad (8)$$

where $[k] = 2k + 1$, $(1/\sigma)({\rm d}\sigma_{kq}/{\rm d}\omega_t)$ is a generalized polarization-dependent differential cross section and $C_{kq}(\theta_r, \phi_r)$ refers to the modified spherical harmonics. In this work, we just calculate the four PDDCSs $(2\pi/\sigma)({\rm d}\sigma_{00}/{\rm d}\omega_t)$, $(2\pi/\sigma)({\rm d}\sigma_{20}/{\rm d}\omega_t)$, $(2\pi/\sigma)({\rm d}\sigma_{22+}/{\rm d}\omega_t)$, and $(2\pi/\sigma)({\rm d}\sigma_{21-}/{\rm d}\omega_t)$, which will be denoted as $P_{00}(\omega_t)$, $P_{20}(\omega_t)$, $P_{22+}(\omega_t)$, $P_{21-}(\omega_t)$ hereafter for simplicity.

2.2. Potential energy surfaces and quasi-classical trajectory calculations

The $^3{\rm A}'$ and $^3{\rm A}''$ PESs employed in our work both have a saddle-point and that on the $^3{\rm A}'$ PES is about 0.2-kcal/mol higher than that on the $^3{\rm A}''$ PES. The $^3{\rm A}'$ barrier height of GLDP (the generalized London–Eyring–Polanyi–Sato double-polynomial methods) is 13.22 kcal/mol and that of $^3{\rm A}''$ is 13.04 kcal/mol. The $^3{\rm A}'$ barrier height of RMOS (the rotating Morse spline) is 13.44 kcal/mol while that of $^3{\rm A}''$ is 13.26 kcal/mol.[18]

Here, the quasi-classical trajectory method is similar to that used previously.[27−29] The collision energies are the same as those in our previous work, which are taken to be 15, 17.5, 20, 22.5, and 25 kcal/mol. In the calculation, a batch of 50000 trajectories is run and each step for integration is chosen to be 0.1 fs. The conservative extent is 10^{-4} eV for total energy and $10^{-5}h$ for total angular momentum. As for the optimization of the impact parameter $b_{\rm max}$, we adopt the same method used by Cao *et al.*[34] and Wang *et al.*[35] That is, we first calculate a small quantity of trajectories at certain fixed values of b and systematically change the value of b until no reactive trajectories are obtained. This b value obtained is then used as the starting value in calculation with large quantities of trajectories. By adjusting the b values several times in a similar way described above for calculation with small quantities of trajectories, we can finally obtain $b_{\rm max}$ that ensures the convergence of the present QCT calculations. Moreover, Wang *et al.*[35] have investigated the reaction $SiH_4 + H \rightarrow SiH_3 + H_2$ on the 12-dimensional *ab initio* Wang–Sun–Bian (WSB) surface. In their work various dynamical quantities are obtained and reaction mechanisms are analysed. Cao *et al.*[34] have studied both the $H + SiH_4$ abstraction and exchange reactions on the accurate global 12-dimensional *ab initio* PES. They investigated the excitation functions and product angular distributions in detail at various collision energies and provided insights into the underlying reaction mechanism. Both calculations adopted the QCT method and considered the quantum-mechanical zero-point energy (ZPE) in the same way, namely a so-called nonactive method, which follows the genuine QCT approach but discards all of the reactive trajectories that fulfill one of the following conditions: (i) the initial total energy is lower than the sum of the classical energy and harmonic ZPE of the saddle point; (ii) the vibrational energy of the products is lower than the sum of their ZPEs.[34,35] In our present study, we also take ZPE correction into account in the QCT calculation.

3. Results and discussions

3.1. Isotope effect at $^3A'$ PES

The $P(\theta_r)$ distributions are shown in Figs. 2(a) and 2(b), which describe the correlation between the $\boldsymbol{j}'$–$\boldsymbol{k}$ vectors. Figure 2(a) is the result taken from our previous work about the reaction $O + H_2$[26] and figure 2(b) is the result of the isotope variant $O + D_2$ in this work. It can be concluded that the product rotational momentum vector $\boldsymbol{j}'$ prefers to align in the direction perpendicular to the reactant relative velocity $\boldsymbol{k}$, because the distributions all have only one peak at $\theta_r = 90°$ and are well symmetric with respect to $\theta_r = 90°$. Furthermore, at each collision energy, the alignment of the isotope variant $O + D_2$ is much more stronger than that of $O + H_2$: although the height of the peak is lower than that of $O + H_2$, its breadth is much bigger than that of $O + H_2$ at the collision energy of 15 kcal/mol, hence the product alignment in isotope variant is still stronger at this collision energy. As for other collision energies, it is no doubt that the alignment of the isotope variant $O + D_2$ is stronger because of the obvious height superiority. The graphs of the values of $\langle P_2(\cos\theta_r)\rangle$ as shown in Fig. 3, which shows the relation with the product rotational alignment, demonstrate a good agreement with the $P(\theta_r)$ distributions. As shown in the figure, all $\langle P_2(\cos\theta_r)\rangle$ values of the isotope variant $O + D_2$ are much more negative than that of $O + H_2$, hence the product rotational momentum $\boldsymbol{j}'$ of the isotope variant $O + D_2$ presents a strongly anisotropic distribution with respect to $\boldsymbol{k}$. Moreover, with increasing collision energy, the degree of anisotropic distribution continues to increase for isotope variant $O + D_2$ which can be observed from the decline of the isotope variant curve. This is in good agreement with the $P(\theta_r)$ distributions of the isotope variant $O + D_2$ as well. Therefore, we can draw the conclusion that there surely exists the mass effect in the product rotational momentum and such a mass effect gets stronger as collision energy increases.

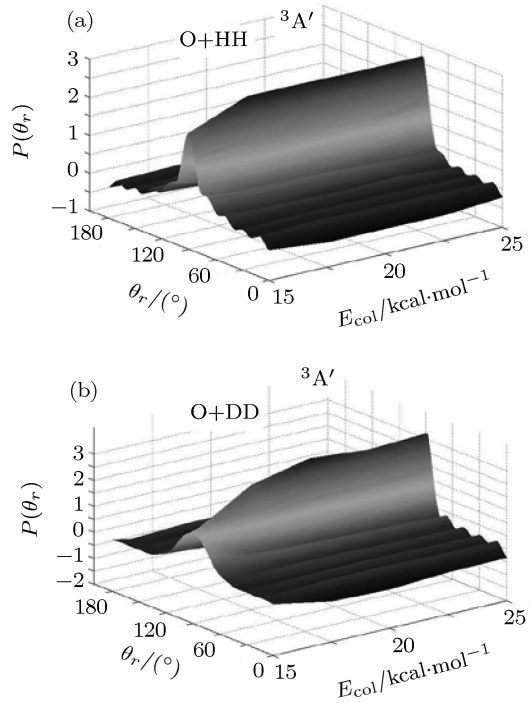


Fig. 2. $P(\theta_r)$ distributions for the reactions (a) $O + H_2$ (results are reported in Ref. [26]) and (b) $O + D_2$ on the $^3A'$ PES.

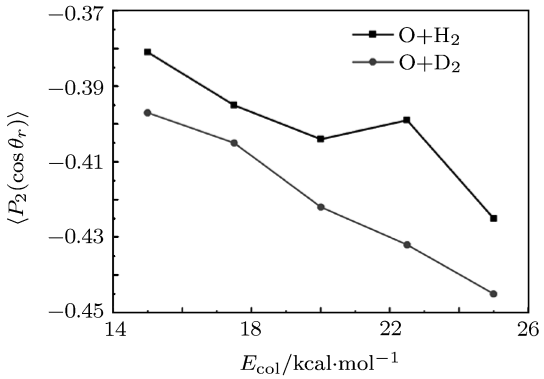


Fig. 3. The relationship between $\langle P_2(\cos\theta_r)\rangle$ and the value of the collision energies for the reactions $O + H_2$ (results reported in Ref. [26].) and $O + D_2$ on the $^3A'$ PES.

$P(\phi_r)$ distributions which describe the $\boldsymbol{k}$–$\boldsymbol{k}'$–$\boldsymbol{j}'$ vector correlations are depicted in Figs. 4(a) and 4(b), in which figure 4(a) is the result of our previous work and figure 4(b) represents the result of the isotope variant $O + D_2$. There are two important common characters in these two reactions $O + H_2$ and $O + D_2$: one is that the $P(\phi_r)$ distributions both have only one peak at the angle around $\phi_r = 270°$, revealing a preference for the left-handed product rotation in the planes parallel to the scattering plane. This surely indicates that all the products are strongly oriented in the direction of the negative y axis, directly reflecting a strong polarization of the product rotational angular momentum. Another common character is that the heights of their peaks first increases and then decreases as collision energy increases, suggesting that the product orientation is correspondingly getting stronger and then weakened as collision energy increases. Moreover, the width of the distribution is always growing as the collision energy goes up, which denotes a change of preference from in-plane mechanism to out-of-plane

mechanism. There also exist some differences between the reactions $O + H_2$ and $O + D_2$. At the collision energy of 15 kcal/mol, the peak of $P(\phi_r)$ distribution of the reaction $O + H_2$ is higher than that of the isotope variant $O + D_2$. Except this situation, the peak of the former is never higher than the peak of the latter at the five collision energies. But an interesting phenomenon is that at 22.5 kcal/mol the $P(\phi_r)$ distributions of the two reactions almost coincide with each other, especially their peaks. It indicates that at high collision energies, the product of the isotope variant $O + D_2$ behaves in a little stronger polarized manner. Generally speaking, these differences in height can be attributed to the isotopic mass effect.

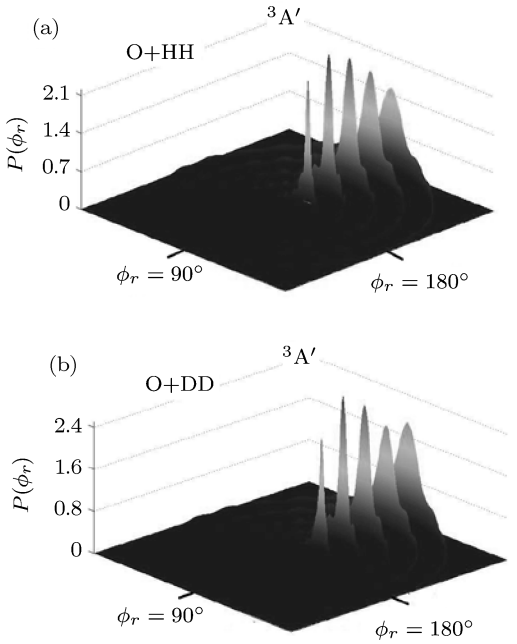


Fig. 4. $P(\phi_r)$ distributions at collision energies of 15, 17.5, 20, 22.5 and 25 kcal/mol from inside to outside respectively for the reactions (a) $O + H_2$ (results reported in Ref [26]) and (b) $O + D_2$ on the ^{3}A′ PES.

Figures 5 plots the four PDDCSs of the reactions $O + H_2$ and $O + D_2$ on the ^{3}A′ PES $P_{00}(\omega_t)$, $P_{20}(\omega_t)$, $P_{22+}(\omega_t)$, and $P_{21-}(\omega_t)$ as functions of collision energy and scattering angle θ_t. In these pictures, figures 5(a)–5(c) show results of our previous work $O + H_2$; and figures 5(d)–5(f) show the results of this work $O + D_2$. first we have a look at $P_{00}(\omega_t)$ and $P_{20}(\omega_t)$ which are correlated with usual differential cross section and expectation value of the second Legendre moment $\langle P_2(\cos\theta_r)\rangle$, respectively. As can be seen, there are both preferred backward scattering and sideways scattering for the reactions $O + H_2$ and $O + D_2$, as they have a peak at the scattering angle between 140° and 180°. But for the isotope variant $O + D_2$, at low collision energy of 15 kcal/mol the peak is much higher (exceed 1.6) than the peak of other energies and its peak is very sharp, unlike that of $O + H_2$, at the same energy. After a careful observation and comparison, discrepancy can be found that sideways scattering range is about 10° narrower for $O + D_2$ which begins to show sideways scattering at $\theta_t = 55°$, while $O + H_2$ begins at $\theta_t = 40°$ at the energies bigger than 17.5 kcal/mol. From the distributions of $P_{20}(\omega_t)$, we can see that the product angular momentum $\boldsymbol{j}'$ is polarized strongly along the direction perpendicular to $\boldsymbol{k}$ at $\theta_t = 180°$ for $O + H_2$ at all collision energies, while it is just the same with the energies 22.5 kcal/mol and 25 kcal/mol for $O + D_2$ because only these energies have peaks at $\theta_t = 180°$. As to $P_{22+}(\omega_t)$, all values of the distributions are negative for all scattering angles revealing a noticeable preference for an alignment of $\boldsymbol{j}'$ along the negative y axis. For $P_{21-}(\omega_t)$ distribution, each of the reactions has one peak at the scattering angle between $\theta_t = 120°$ and 160°. An eminent difference is that for $O + H_2$ when θ_t is between 0° and 70°, the corresponding values are almost zero, while for $O + D_2$ the range of the scattering angle is from 0° to 100°. This suggests that the range of isotropic distribution is wider for $O + D_2$. In other scattering angles as one peak emerges among them, anisotropy of production scattering distribution does exist.

3.2. Isotope effect at ^{3}A″ PES

The $P(\theta_r)$ distributions on ^{3}A″ PES are presented in Fig. 6 which contains results of our previous work $O + H_2$ (Fig. 6(a)) and also the results of the present work $O + D_2$ (Fig. 6(b)). Common characters of these two distributions are not going to be discussed as they are the same as that on ^{3}A′ PES. For this PES, peaks of $P(\theta_r)$ distributions are always higher for the isotope variant $O + D_2$ at all collision energies. In addition, the breadths of their peaks at same collision energy almost coincide with each other. Therefore the degree of product rotational alignment (perpendicular to $\boldsymbol{k}$) effect is always stronger for the isotope variant $O + D_2$ than $O + H_2$. This also can be seen from Fig. 7 in which values of $\langle P_2(\cos\theta_r)\rangle$ are much more negative for $O + D_2$ than those of $O + H_2$. It also indicates that the product rotational momentum $\boldsymbol{j}'$ has a stronger anisotropic distribution with respect to $\boldsymbol{k}$ for $O + D_2$. And these differences must have relations to the isotope mass effect. Common characters about

$P(\phi_r)$ distributions are ignored as well because they are the same as those on $^3A'$ PES. By comparison between Figs. 8(a) and 8(b), we found that the peaks of $P(\phi_r)$ distributions are higher for $O + D_2$ than those of $O + H_2$ at collision energies of 15, 17.5, 22.5 and 25 kal/mol. However, at 20 kcal/mol an interesting phenomenon is that the peaks of $P(\phi_r)$ distributions have equal heights. Thus, it can be concluded that in the range of 15 kcal/mol to 25 kcal/mol the product rotational angular momentum oriented along the negative y axis much more strongly for the variant $O + D_2$ in most collision energies except those around 20 kcal/mol.

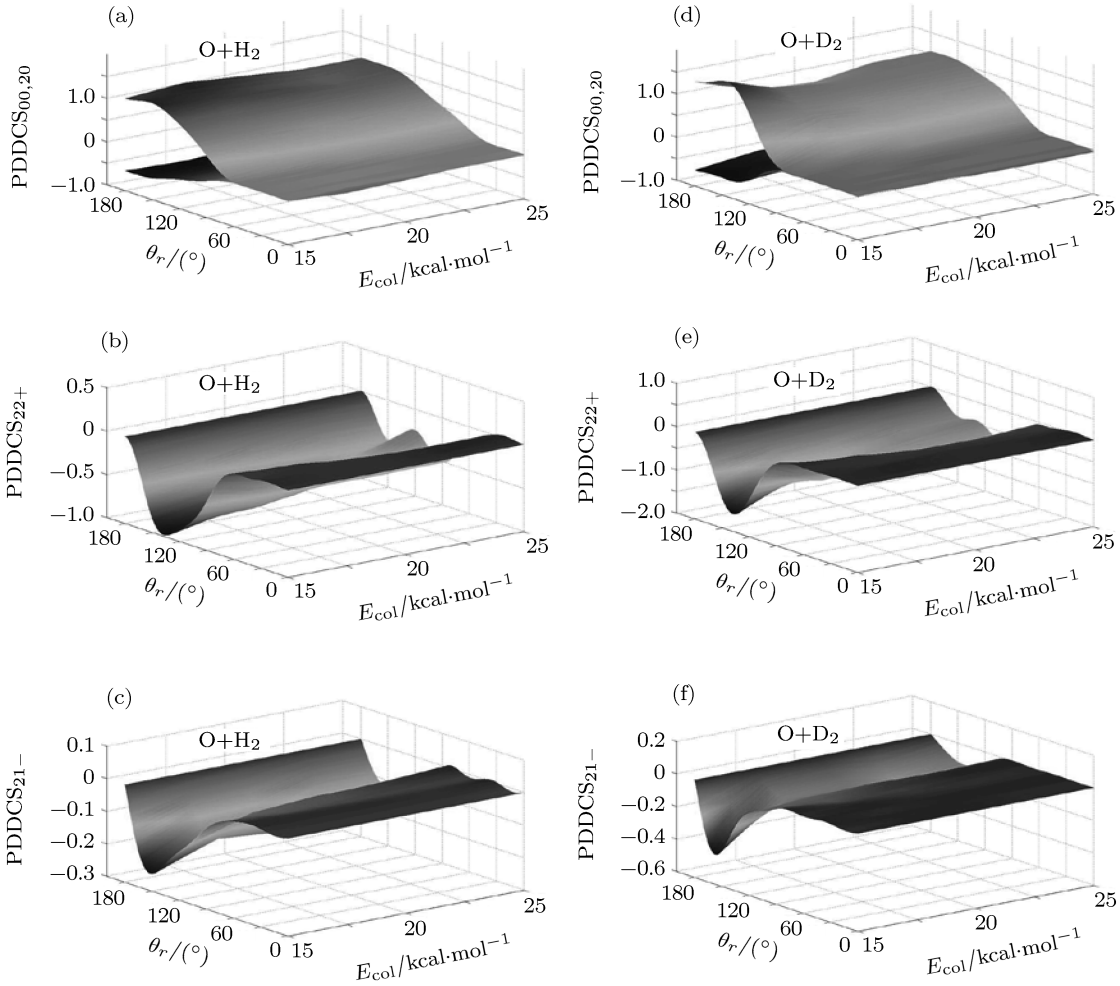


Fig. 5. PDDCSs for the reactions $O + H_2$ in (a), (b), and (c) (results reported in Ref. [26]) and $O + D_2$ in (d), (e), and (f) on the $^3A'$ PES.

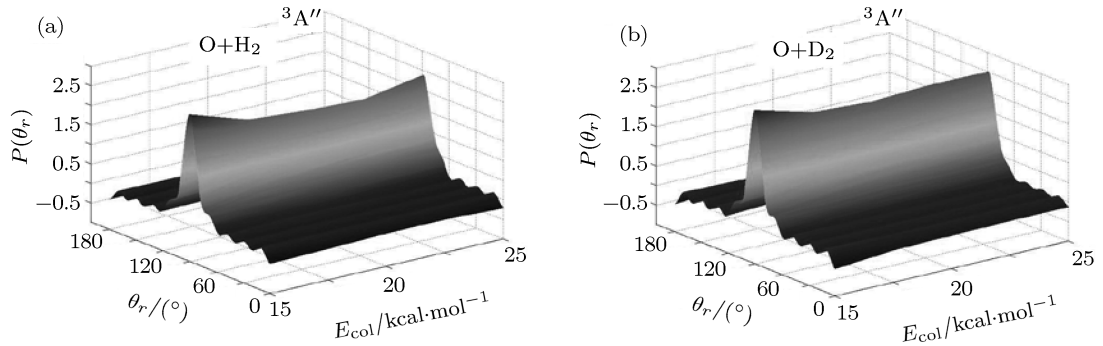


Fig. 6. $P(\theta_r)$ distributions for the reactions $O + H_2$ (a) (results reported in Ref. [26]) and $O + D_2$ (b) on the $^3A''$ PES.

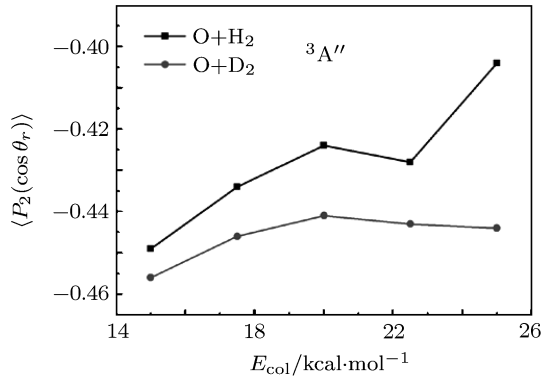


Fig. 7. The relationship between $\langle P_2(\cos\theta_r)\rangle$ and the value of the collision energies for the reactions $O + H_2$ (results reported in Ref. [26]) and $O + D_2$ on the $^3A''$ PES.

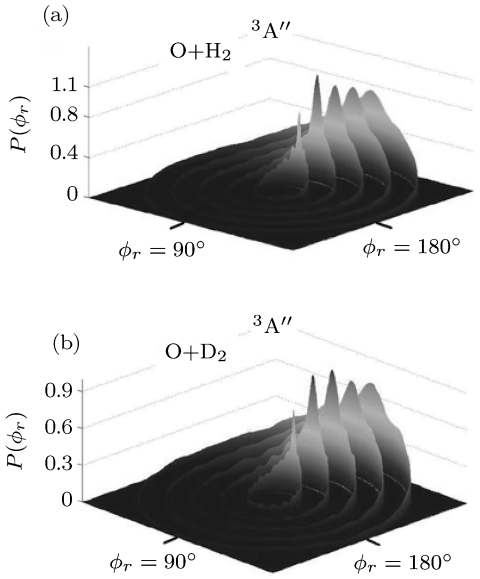


Fig. 8. The $P(\phi_r)$ distributions at collision energies of 15, 17.5, 20, 22.5, and 25 kcal/mol from inside to outside respectively for the reactions $O + H_2$ (a) (results reported in Ref. [26]) and $O + D_2$ (b) on the $^3A''$ PES.

PDDCSs on $^3A''$ PES are depicted in Fig. 9. $P_{00}(\omega_t)$ distributions of the two reactions are alike to some degree: they both have strong backward and sideways scatterings and as the collision energy increases, backward scattering weakens and sideways scattering gradually becomes dominant. This can be seen from that the movement of the peak for low-energy $P_{00}(\omega_t)$ distributions at scattering angle $\theta_t = 180°$, while it moves towards $\theta_t = 90°$–$100°$ gradually. The difference between the reactions is that for each collision energy the peaks of $O + D_2$ move hysteretically than those of $O + H_2$. The calculated $P_{22+}(\omega_t)$ distributions at both reactions show a strong scattering-angle-dependent behaviours with fluctuation over the range of scattering angle.

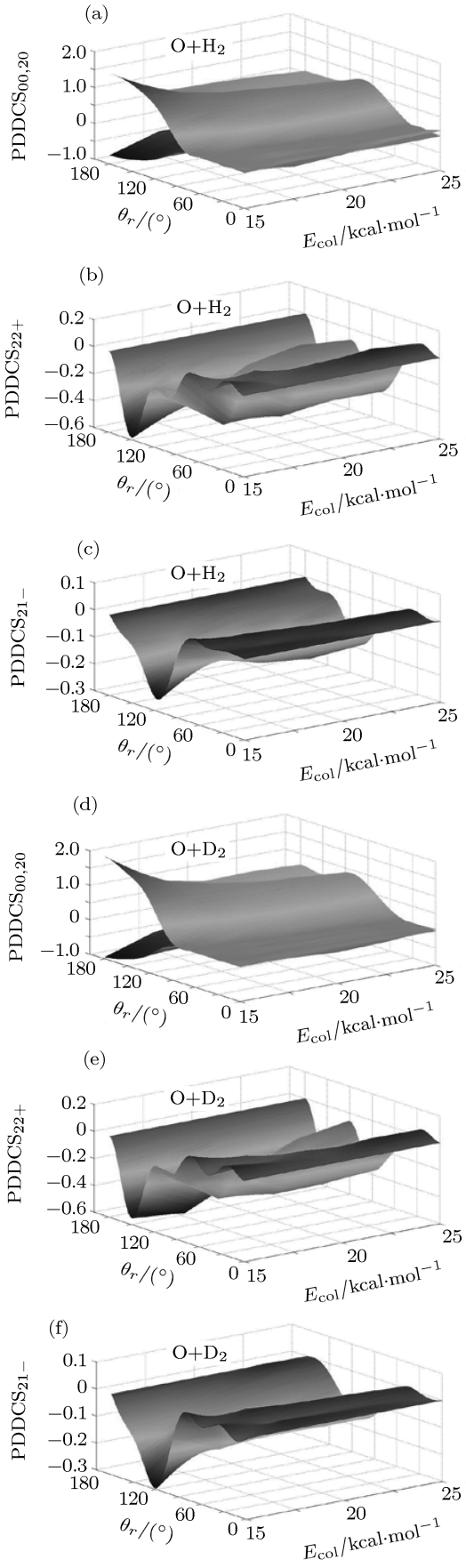


Fig. 9. PDDCSs for the reactions $O + H_2$ in (a), (b), and (c) (results reported in Ref. [26]) and $O + D_2$ (d), (e), and (f) on the $^3A''$ PES.

For $P_{21-}(\omega_t)$, an obvious difference is that the peak has the biggest absolute value near 0.27 at 15 kcal/mol of the reaction $O + H_2$, while that of $O + D_2$ almost reaches 0.3 at 22.5 kcal/mol. This means that the products of the two reactions have the strongest anisotropic distributions at different collision energies.

4. Conclusions

In this work, the title reaction $O(^3P) + D_2$ ($v = 0$, $j = 0$) $\rightarrow$ $OD + D$ has been studied by the QCT method on the $^3A'$ and $^3A''$ PESs. Stereodynamics information about the vector correlations has been obtained through the calculation. In order to investigate the influence of the isotope mass effect, comparison between the present results and our previous results for $O + H_2$ has been made. We found that the isotope mass effect has evident influence in the polarizations of the products on both PESs. Also we concluded that the isotope mass effect differs on the two PESs: the isotope mass effect has stronger influence on $P(\theta_r)$ and PDDCSs of $^3A'$ PES, while the opposite on $P(\phi_r)$ of $^3A''$ PES.

Acknowledgements

The authors thank Prof. Han Ke-Li for providing the stereodynamics QCT code and thank Dr. Chu Tian-Shu for providing the potential energy surface.

References

[1] Zhang X and Han K L 2006 *Int. J. Quantum Chem.* **106** 1815
[2] Hu J, Han K L and He G Z 2005 *Phys. Rev. Lett.* **95** 123001
[3] Zhang H, Zhu R S, Wang G J, Han K L, He G Z and Lou N Q 1999 *J. Chem. Phys.* **110** 2922
[4] Braunstein M, Sdler-Golden S, Maiti B and Schatz G C 2004 *J. Chem. Phys.* 120 4316
[5] Wang W L, Rosa C and Brandão J 2005 *Chem. Phys. Lett.* **418** 250
[6] Li R J, Han K L, Li F E, Lu R C, He G Z and Lou N Q 1994 *Chem. Phys. Lett.* **220** 281
[7] Chen Y T, Zhang W P, Wang X Q and Zhao G J 2009 *Chem. Phys.* **365** 158
[8] Liu Y F, Gao Y L, Shi D H and Sun J F 2009 *Chem. Phys.* **364** 46
[9] Hou C Y, Li Y M and Zhao D 2009 *Chem. Phys.* **364** 64
[10] Han B, Zong F J, Wang C L, Ma W Y and Zhou J H 2009 *Chem. Phys.* **374** 94
[11] Chu T S and Han K L 2005 *J. Phys. Chem.* A **109** 2050
[12] Chu T S, Zhang X and Han K L 2005 *J. Chem. Phys.* **122** 214301
[13] Chu T S, Zhang Y and Han K L 2006 *Int. Rev. Phys. Chem.* **25** 201
[14] Chu T S and Han K L 2008 *Phys. Chem. Chem. Phys.* **10** 2431
[15] Li B and Han K L 2009 *J. Phys. Chem.* A 113 10189
[16] Song J B and Gislason E A 1996 *J. Chem. Phys.* **105** 10429
[17] Song J B and Gislason E A 1996 *Chem. Phys. Lett.* **258** 260
[18] Rogers S, Wang D, Kuppermann A and Walch S 2000 *J. Phys. Chem.* A **104** 2308
[19] Wei Q, Li X and Li T 2010 *Chem. Phys.* **368** 58
[20] Wei Q, Li X and Li T 2009 *Chin. J. Chem. Phys.* **22** 523
[21] Weck P F and Balakrishnan N 2005 *J. Chem. Phys.* **123** 144308
[22] Weck P F, Balakrishnan N, Brandão J, Rosa C and Wang W 2006 *J. Chem. Phys.* **124** 074308
[23] Martínez R, Sierra J D and González M 2005 *J. Chem. Phys.* **123** 174312
[24] Rio C M A and Brandão J 2007 *Chem. Phys. Lett.* **433** 268
[25] Carrasco S G, Sánchez L G, Aguado A, Roncero O, Alvariño J M, Hemández M L and Paniagua M 2004 *J. Chem. Phys.* **121** 4605
[26] Xu Z H and Zong F J 2010 *J. Mol. Struc. Theochem* **960** 22
[27] Wang M L, Han K L and He G Z 1998 *J. Phys. Chem.* A **102** 10204
[28] Han K L, He G Z and Lou N Q 1996 *J. Chem. Phys.* **105** 8699
[29] Wang M L, Han K L and He G Z 1998 *J. Chem. Phys.* **109** 5446
[30] Chen M D, Han K L and Lou N Q 2002 *Chem. Phys. Lett.* **357** 483
[31] Li J L, Yong Q, Ma F C, Ni Y Q and Zhao L N 2008 *Chin. Phys.* B **17** 3649
[32] Han J R, Liu X F, Wang Y J, Wang Y Z, Xu G Y and Yang L 2008 *Chin. Phys.* B **17** 4158
[33] Wong C Y, Lee T G and Wang L S 2008 *Chin. Phys.* B **17** 2897
[34] Cao J W, Zhang Z J, Zhang C F, Liu K, Wang M H and Bian W S 2009 *Proc. Natl. Acad. Sci. USA* **106** 13180
[35] Wang M H, Sun X M and Bian W S 2008 *J. Chem. Phys.* **129** 084309